Article ID: 1006-8775(2012) 03-0284-13

VALIDATION OF NEAR-SURFACE WINDS OBTAINED BY A HYBRID WRF/CALMET MODELING SYSTEM OVER A COASTAL ISLAND WITH COMPLEX TERRAIN

LU Yi-xiong (路屹雄)[1], TANG Jian-ping (汤剑平)[1], WANG Yuan (王　元)[1], SONG Li-li (宋丽莉)[2]

(1. School of Atmospheric Sciences, Nanjing University, Nanjing 210093 China; 2. Climate Center of Guangdong Province, Guangzhou 510080 China)

Abstract: The results from a hybrid approach that combines a mesoscale meteorological model with a diagnostic model to produce high-resolution wind fields in complex coastal topography are evaluated. The diagnostic wind model (California Meteorological Model, CALMET) with 100-m horizontal spacing was driven with outputs from the Weather Research and Forecasting (WRF) model to obtain near-surface winds for the 1-year period from 12 September 2003 to 11 September 2004. Results were compared with wind observations at four sites. Traditional statistical scores, including correlation coefficients, standard deviations (SDs) and mean absolute errors (MAEs), indicate that the wind estimates from the WRF/CALMET modeling system are produced reasonably well. The correlation coefficients are relatively large, ranging from 0.5 to 0.7 for the zonal wind component and from 0.75 to 0.85 for the meridional wind component. MAEs for wind speed range from 1.5 to 2.0 m s^{-1} at 10 meters above ground level (AGL) and from 2.0 to 2.5 m s^{-1} at 60 m AGL. MAEs for wind direction range from 30 to 40 degrees at both levels. A spectral decomposition of the time series of wind speed shows positive impacts of CALMET in improving the mesoscale winds. Moreover, combining the CALMET model with WRF significantly improves the spatial variability of the simulated wind fields. It can be concluded that the WRF/CALMET modeling system is capable of providing a detailed near-surface wind field, but the physics in the diagnostic CALMET model needs to be further improved.

Key words: near-surface winds; WRF/CALMET modeling system; complex terrain

CLC number: P435 **Document code:** A

1 INTRODUCTION

The accurate assessment of wind energy potential calls for developing better methods of producing high-resolution wind fields. For designing wind power plants and micrositing of wind turbines, detailed spatial characteristics of the wind field are desired, particularly in areas of complex terrain. The regional representation of local field measurements highly depends on the quality and availability of wind records. Topography also increases the complexity of the flow as a consequence of its dynamic and thermal effects[1-4]. Generally, mesoscale meteorological models are used to deduce the near-surface wind field in complex terrain by dynamical downscaling of reanalysis data. A typical jump in the horizontal resolution is from about one to two degrees down to a few kilometers. For example, Rife et al.[5] downscaled the 40-km Eta model analyses onto the domain with a 1.33-km grid increment for the area of the Salt Lake valley and surrounding mountains, using the fifth-generation Pennsylvania State University-National Center for Atmospheric Research Mesoscale Model (MM5). It was found that the 1.33-km MM5 was capable of reasonably representing the complex terrain of the Salt Lake City region and corresponding influences on the local circulation patterns. The ALADIN (a high resolution numerical prediction project) model was applied in the study of Žagar et al.[6] to downscale the 40-yr European Centre for Medium-Range Weather Forecasts (ECMWF) Re-Analysis (ERA40) data onto a 10-km grid covering the complex terrain of Slovenia. The simulated wind field at 10 m above ground level (AGL) was compared with the observations at 11 sites, and the results showed that the model performed best at mountaintop sites. Jiménez et al.[7] also downscaled the ERA40 data for the period 1992–2005 using the

Received 2011-03-09; **Revised** 2012-06-14; **Accepted** 2012-07-15

Foundation item: National Public Benefit Research Foundation of China (2008416048; GYHY201006035)

Biography: LU Yi-xiong, Ph.D. candidate, primarily undertaking research on numerical simulation of boundary-layer meteorology.

Corresponding author: TANG Jian-ping, e-mail: jptang@nju.edu.cn

Weather Research and Forecasting (WRF) model with a 2-km resolution to investigate the daily-mean wind variability over the Iberian Peninsula. Wind observations were divided into four subregions with similar temporal wind variability. The simulated variability at the four subregions was similar to that found in the observations, and the meridional wind variability was reproduced more accurately than the zonal wind. More detailed descriptions of the aforementioned studies can be found in the literatures. These studies are briefly reviewed here to illustrate the effectiveness of the dynamical downscaling as a tool for analyzing high-resolution wind fields using meteorological mesoscale models. Model results can provide three-dimensional wind field structures that cannot be obtained from field measurements. They can describe the changes induced on the wind field from the topography and land cover variations. Moreover, model-based approaches allow for a more complete understanding of the physical processes and mechanisms that impact the wind variability.

More recently, the hybrid approach is increasingly being used by combining a mesoscale prognostic model with a diagnostic meteorological model. The mesoscale model accounts for treating dynamic effects on scales of several kilometers, and the diagnostic model is defined on a grid with much finer resolution to address smaller-scale topographic effects (Ludwig et al.[8]). This hybrid approach is considered practical enough to provide finer details of wind fields in complex terrain, with acceptable computational requirements. One of the most prominent examples is the MM5/California Meteorological Model (CALMET) modeling system[9-11]. Yim et al.[11] investigated the wind energy potential in Hong Kong by producing high-resolution wind maps for the entire year of 2004 using the hybrid MM5/CALMET system. The MM5 simulations were performed on four nested grids at horizontal resolution from 40.5 km down to 1.5 km, and the CALMET model was run in a domain with a fine resolution of 100 m. The MM5 model outputs were ingested into the CALMET model, and CALMET adjusted the mesoscale winds to the finer-resolution topography. Subsequently, the model results were integrated with extensive field measurements from forty-one surface sites and one upper air sounding site in the objective analysis procedure of CALMET. The wind observations were blended with model results based on an inverse-distance-squared interpolation scheme. The final results indicated that this hybrid MM5/CALMET system could generate accurate wind fields for evaluation of wind energy resources in Hong Kong with an extremely complex topography. However, the overall performance of the CALMET model may be contributed by the objective analysis procedure, rather than the physical adjustments for the finescale terrain effects. The performance of CALMET treating terrain effects without measurements intervention was not rigorously evaluated. Obviously, the reliability of the objective analysis depends upon the density, frequency, and accuracy of the observations, but studies are often undertaken over a region with complex topography where limited or no observations are available. It is intended to lean on the ability of the model to deduce its own near-surface wind field structures. In this paper, the study area encompasses Hailing Island, on the coast of South China Sea. Elevations range from sea level to over 360 m; several small hills are located on the Hailing Island. The mesoscale WRF model is employed to provide the coastal weather conditions over this tropical region. The CALMET model is expected to resolve the microscale terrain effects of Hailing Island. The main purpose of this study is to evaluate the simulated winds produced by the hybrid WRF/CALMET modeling system. The objectives are 1) to verify the performance of the WRF/CALMET system in terms of traditional verification statistics and wind variability spectra, 2) to evaluate the existing physical terrain treatments in CALMET, and describe the degree to which the accuracy of the wind simulations can be improved by CALMET without objective analysis, and 3) to describe the CALMET's accuracy relative to the initialization by WRF outputs, and determine whether it is required that the WRF model should be run at the highest possible horizontal resolution.

The paper is organized as follows. Details of experimental design are presented in Section 2. The observational data used for model validation and the verification strategies are also presented in this section. Results are discussed in Section 3. First the performance of the hybrid modeling system is validated in terms of traditional scores, and then the verification is undertaken in spectral domains. The spatial variation of the simulated wind fields obtained by the WRF/CALMET system is also discussed. At last, the main conclusions and discussion are summarized in Section 4.

2 EXPERIMENTAL DESIGN

2.1 *Mesoscale model WRF*

The prognostic mesoscale model used in this study is the Weather Research and Forecasting (WRF) model version 3.1.1, developed by the National Center for Atmospheric Research (NCAR). WRF has been a widely used community model designed to simulate mesoscale and regional-scale atmospheric circulations (Skamarock et al.[12]). Good performances have been proved in previous studies[13-17]. In this study, the WRF model was configured with four one-way nested domains with horizontal grid spacing of 27 (D1; mesh size of 180×130), 9 (D2; mesh size of

193×154), 3 (D3; mesh size of 175×175), and 1 (D4; mesh size of 82×82) km, respectively (Figure 1). The outermost 27-km domain covers most of southeastern China and South China Sea to capture the synoptic-scale features, whereas the innermost 1-km domain covers Hailing Island and its vicinity and is designed to resolve the local-scale circulation features. In the vertical direction, 35 full Eta levels from the surface to 100 hPa were defined on a non-uniform vertical grid, with the lowest 12 levels below 1 km to resolve the detailed structure of the planetary boundary layer (PBL).

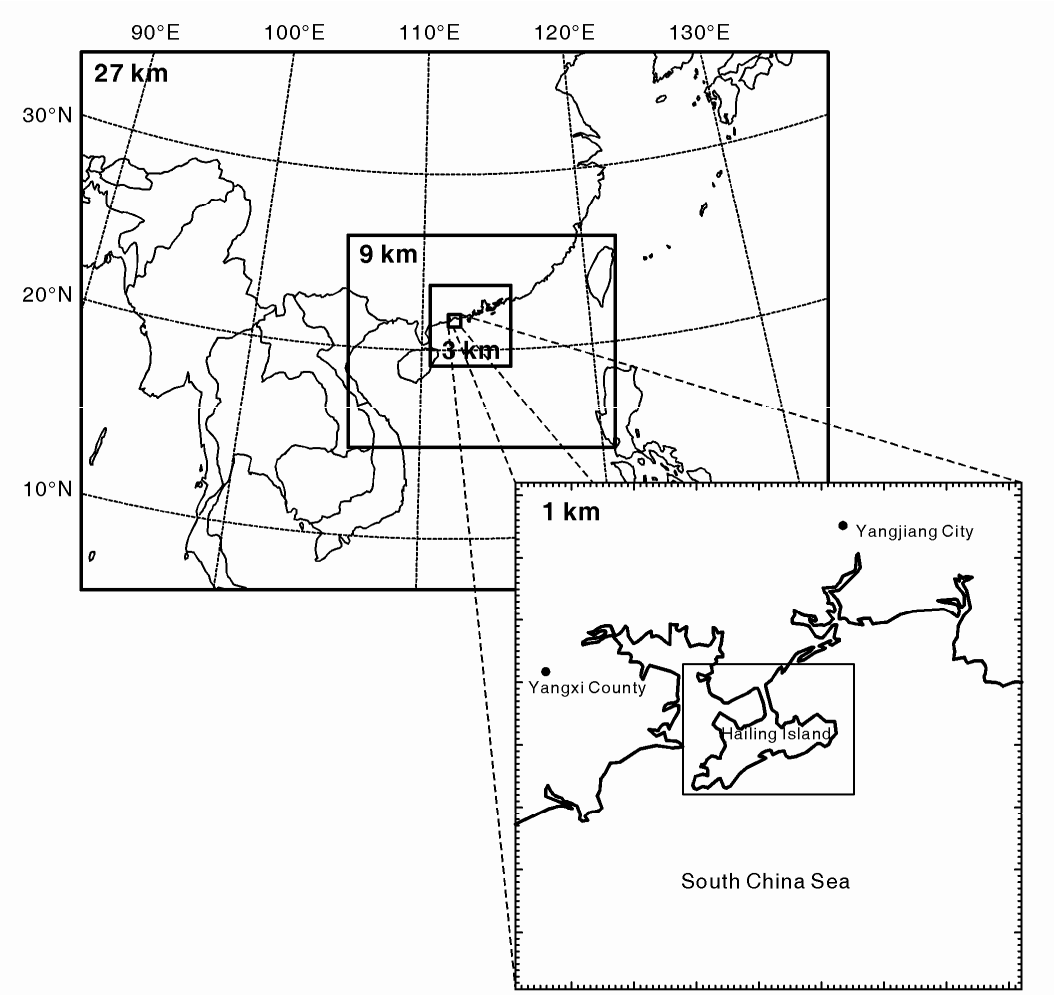

Figure 1. Area coverage for the four nested grids in the WRF model. The grid increment for each grid is indicated. The expanded innermost grid shows the shoreline and the location of the Hailing Island. The box in the innermost grid indicates the study region, which is also the computational domain in the CALMET model.

The Single-Moment 3-class simple ice scheme was applied in all domains for microphysical parameterization (Hong et al.[18]). The Kain-Fritsch cumulus scheme was used in D1 and D2 (Kain[19]), and explicit convection was calculated in D3 and D4. Shortwave radiation processes were parameterized using the Dudhia scheme (Dudhia[20]) and the Rapid Radiative Transfer Model (Mlawer et al.[21]) was applied for longwave radiation processes. The Yonsei University (YSU) PBL scheme was used for the PBL scheme (Hong et al.[22]). Finally, the Noah land surface model was used. The topographic data were obtained from the U.S. Geological Survey (USGS) global 30 arc-seconds elevation (GTOPO30) dataset, and the 20-category MODIS-based land use data were used to determine the surface physical properties.

In recent years, climatological studies have shown that mesoscale models perform better in a reinitialized short-term integration mode than in a continuous long-term integration mode[23-25]. In the present study, a 1-year data set of wind simulations were obtained by multiple short WRF runs. For each run on the four nested domains, D1 was initialized as a “cold start” at 0600 UTC and run for 48 h. The initial conditions were provided by the 1.125° European Centre for Medium-Range Weather Forecasts (ECMWF) - Tropical Ocean and Global Atmosphere (TOGA) global analyses. The inner domains (D2, D3 and D4) were started every 6 hours and ended at the same time as D1. Therefore, D4 was started at 0000 UTC and

run for 24 h. The initial fields of each inner domain, interpolated from its mother domain, are expected to contain more mesoscale information. Moreover, WRF has four-dimensional data assimilation (FDDA) capacities based on nudging techniques. In the current study, only grid nudging was applied to the outermost domain (D1) to improve the accuracy of the synoptic-scale background flow. Neither grid nudging or observational nudging was applied to D2, D3 and D4 to retain the ability of the WRF model to generate its own mesoscale features.

2.2 *Diagnostic model CALMET*

The diagnostic meteorological model used in this study is the California Meteorological Model (CALMET) version 6.326, which is the meteorological component of the California Puff (CALPUFF) dispersion modeling system (Scire et al.[26]). The diagnostic CALMET uses a two-step approach to compute the wind fields. In the first step, an initial-guess wind field is adjusted for kinematic effects of terrain, slope flows, and terrain blocking effects to produce a Step 1 wind field. The second step consists of an objective analysis procedure to introduce observational data into the Step 1 wind field to produce a final wind field.

In this present study, the Universal Transverse Mercator (UTM) grid system was used in CALMET and the computational domain was set up with 261×201 grid points with 100 m grid spacing (Figure 2). CALMET is written with terrain-following vertical coordinates and the vertical coordinates were set with 22 levels, including 10, 20, 30, 40, 50, 60, 70, 80, 90, 100, 110, 120, 130, 140, 150, 200, 300, 400, 550, 700, 850 and 1000 m. The objective analysis procedure was not used. The major part of this paper is concerned with the evaluation of the terrain-adjusted Step 1 wind field. The terrain in CALMET was constructed using the National Aeronautics and Space Administration (NASA) Shuttle Radar Topography Mission 3 arc-seconds (SRTM3) terrain data. As shown in Figure 3, the topographic features of Hailing Island are more detailed as the grid size decreases from 3 km to 100 m. The CALMET computations in this study could be regarded as an attempt to compensate for the difference between the mesoscale model and the actual terrain elevations.

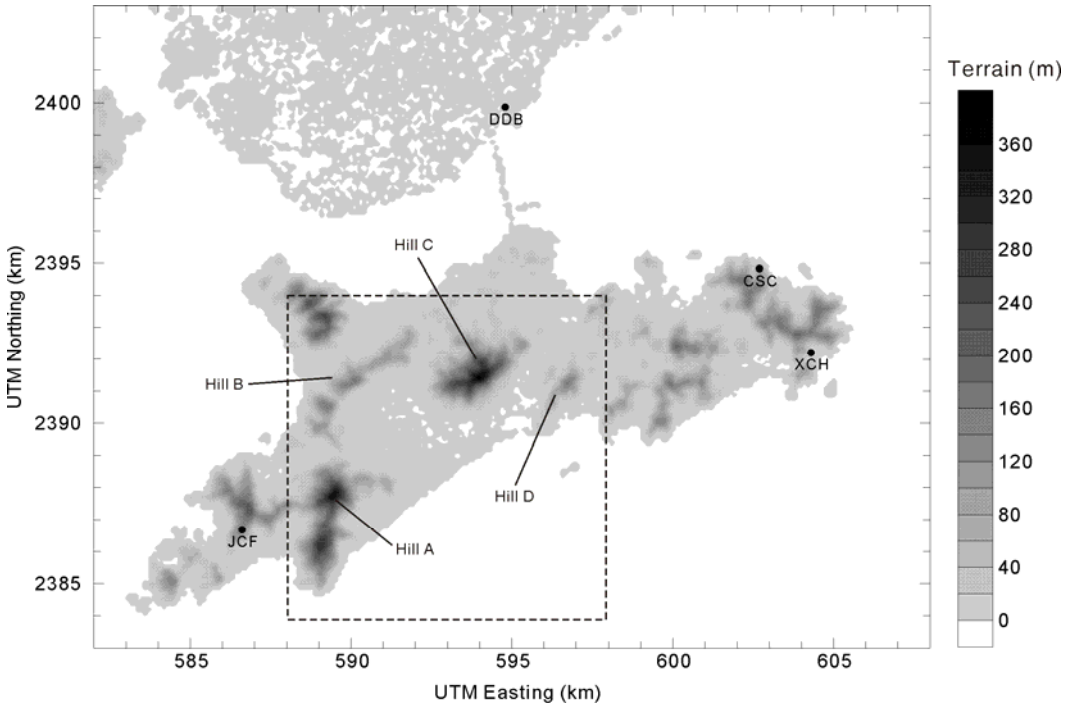

Figure 2. Computational domain in CALMET (area in the box shown in Figure 1). The shaded contours represent the terrain elevations. The four wind measurement masts are indicated by solid dots with their corresponding names. The dashed box enclosing four major hills indicates the region discussed in Section 3.3.

WRF generates a vertical profile of winds over each grid point. The CALMET model contains an option to allow the WRF profile to serve as the initial-guess field. The first step is to interpolate the gridded mesoscale winds to the CALMET horizontal and vertical grids. The linear interpolation is performed to convert winds at the mesoscale model's vertical levels to the CALMET levels. An inverse-distance-squared weighting procedure is used in the horizontal to interpolate the mesoscale model winds to the CALMET grid points. In the present study, WRF profiles in 3-km D3 and 1-km D4 were

used as input to CALMET, respectively.

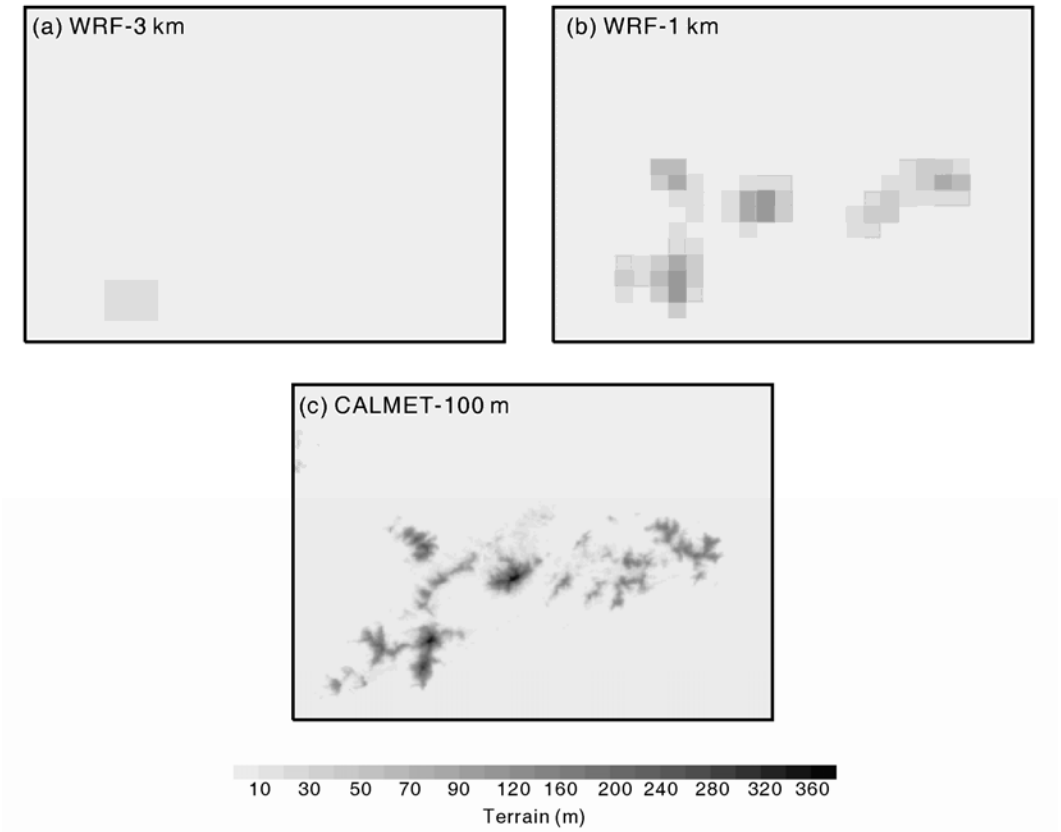

Figure 3. Orography of Hailing Island as represented by (a) the WRF model with 3-km horizontal resolution, (b) the WRF model with 1-km horizontal resolution, and (c) the CALMET model with 100-m horizontal resolution.

2.3 *Data preparation*

The simulated wind time-series were obtained by 1) the 3-km WRF, denoted as W3km, 2) the 1-km WRF, denoted as W1km, 3) the 3-km WRF coupled with the 100-m CALMET, denoted as W3km/C100m, and 4) the 1-km WRF coupled with the 100-m CALMET, denoted as W1km/C100m, respectively. The model output was saved every hour. So the simulated time series consists of hourly instantaneous wind speed. The simulated wind speed at a site was selected at a point which best corresponds to the surrounding orography, among the four neighboring grid points. On the other hand, the observational data were collected from four wind measurement masts (Figure 2). The wind speed and direction were recorded as an integrated average for every 10-min interval at both 10 m and 60 m AGL. The records at the top of every hour were used as validation data. Both the observed and simulated time-series covered the period from 12 September 2003 to 11 September 2004. The validation period includes all seasons with a chance of covering most of the typical meteorological situations, so it could be expected to describe the surface wind climatology over the study area.

3 RESULTS

3.1 *Traditional verification statistics*

A basic visual assessment of the wind speed distribution conveys a first impression of the simulation accuracy. Figures 4 and 5 show boxplots of wind speed simulations made by the WRF/CALMET system, together with the corresponding observations. Boxplots provide a means of examining the location, spread and skewness of the observations and the simulations. The box covers the central 50% of the data, and the line across the center of the box indicates the median. The whiskers attached to the box show the range of the data, from minimum to maximum. At 10 m AGL, the medians of the simulated winds are near the observed; whereas the simulated medians generally present a shift to the high winds at 60 m AGL. The spread of the simulations is less than the spread of the observations at 10 m AGL, especially at the sites of DDB and CSC. The simulated maximal wind speeds are 6 m s^{-1} and 3 m s^{-1} less than the observed maxima at DDB and CSC, respectively. However, the extreme winds are simulated better at 60 m AGL, excluding DDB.

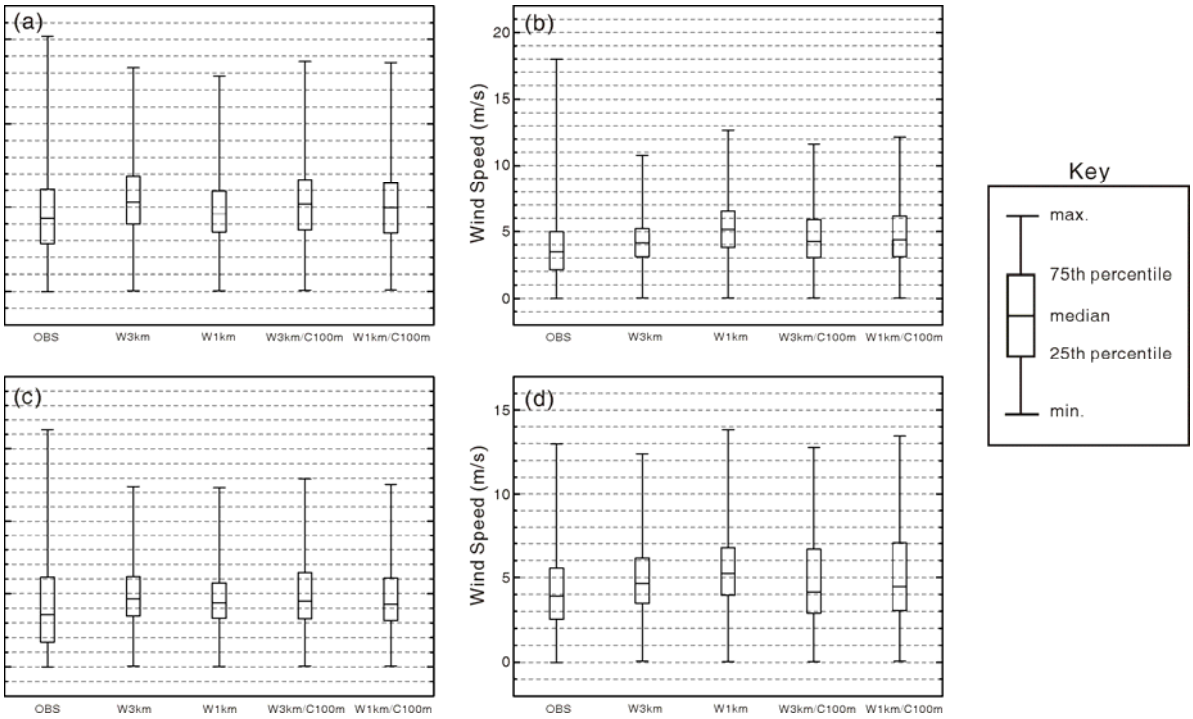

Figure 4. Boxplots of the wind speed simulations and the corresponding observations at 10 m AGL for sites of (a) JCF, (b) DDB, (c) CSC and (d) XCH in the 1-year period.

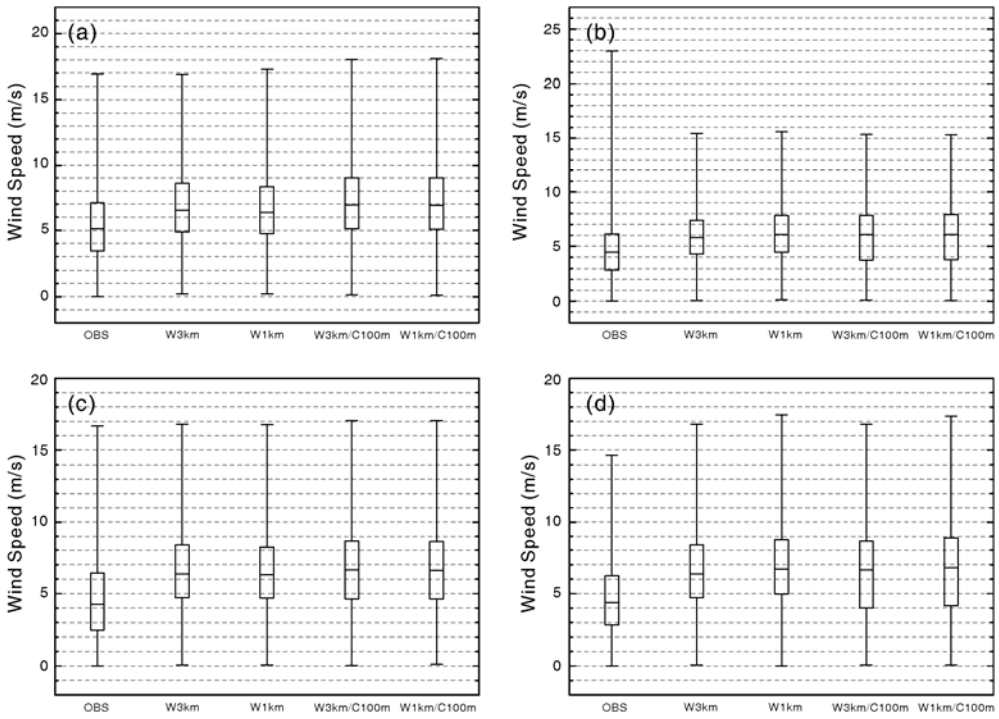

Figure 5. Same as Figure 4 but at 60 m AGL.

The quantitative comparison between simulated and observed winds was then performed using Taylor diagram (Taylor[27]). The Taylor diagram is a polar plot. The angle depicts correlation ranging from 0 to 1. The radial coordinate represents the standard deviation (SD), normalized by the observed SD. Hence, the unit point at the abscissa indicates observations. Because the SDs of the two time series and their correlation are related with the root-mean-square error (RMSE) of the anomalies by the law of cosines, the RMSE of anomalies is proportional to the radial distance from the unit point. Figure 6 shows Taylor diagrams calculated with the simulated and observed wind components for each

site. The good performance of the WRF/CALMET system could be demonstrated by the relatively large correlation. Rife et al.[5] proposed that a value of 0.4 is appropriate to represent the subjective cutoff for "useful" near-surface wind field forecast skill. In Figure 6, the correlation coefficients are above 0.5 for both zonal and meridional wind components. The maximum (0.84) is reached at the CSC site for the 60-m-AGL meridional wind component. The meridional wind is reproduced more accurately than the zonal wind, which is consistent with the results found by Jiménez et al.[7]. In particular, the correlation ranges from 0.52 to 0.71 for the zonal wind component, whereas it ranges from 0.75 to 0.84 for the meridional wind component. For the 10-m-AGL zonal wind, the SDs are generally underestimated, while the SDs of the zonal wind at 60 m AGL are overestimated. For the meridional wind, the SDs are overestimated at both 10 m and 60 m AGL. Moreover, there is no consistent tendency for the errors to decrease with increased horizontal resolution, leading to the counterintuitive fact that wind simulations do not generally improve with higher resolution. Actually, the statistical improvements are minimal with a reduction in grid spacing from 3 to 1 km in WRF. The skill scores are contaminated somewhat by the CALMET computations. An example of this is that the W3km time-series are the best estimates for the 10-m-AGL zonal wind component.

Figure 7 summarizes the diurnal variations of the mean absolute errors (MAEs) for wind speed and direction. MAEs for wind direction range from 30 to 40 degrees. Interesting features of the MAEs for wind direction are the two maxima around 0300 UTC (1100 LST) and 2000 UTC (0400 LST), respectively. The transition between sea breeze and land breeze usually happens at these times. It may be that the WRF model does not adequately represent the complex transition processes. The near-surface wind field is highly variable over the coastal region during these transition periods. The MAEs for the 10-m wind speed range from 1.7 to 2.1 m s^{-1}, whereas they are about 0.5 m s^{-1} larger at 60 m AGL. In addition, it can be found that the errors are enlarged with finer grid resolution. In fact, the wind speed estimates from W3km are the best with smallest MAEs. Although the topographic features are resolved more realistically with finer grids, increasing horizontal resolution does not necessarily produce more skillful statistical scores (Mass et al. [28]).

3.2 *Spectral analysis*

In the study of Rife et al.[5], the circulation scales were grouped into three period bands: the diurnal period of 22-26 h, the subdiurnal period, and the longer-than-diurnal (LTD) period. The mesoscale and smaller scale flows could be quantitatively defined by the power in the diurnal and subdiurnal components of the wind time-series. For this purpose, the wind speed time series were decomposed by the spectral analysis method based on the discrete fast Fourier transform (Ghil et al.[29]). As shown in Figure 8, the spectral curves do not vary much with location. All the four sites have a large amount of LTD power, which may be considered with synoptic scale motions. Furthermore, the power curves present two maxima around the periods of 24 h and 12 h, respectively, indicating that the motions with diurnal and subdiurnal scales are evident in the study area.

A common action of model dynamics and physics at a finer resolution enhances the temporal variability. Downscaling by the WRF/CALMET modeling system introduces new scales. It is desired that the WRF/CALMET system have its spectral power distribution as close as the observed distribution, and the amount of power in each time range as similar as possible to the measured amount. These expectations are checked in Figure 9. The LTD and diurnal bands are reproduced reasonably well. The largest discrepancy between the WRF/CALMET results and observations is found in the subdiurnal range. The motions with subdiurnal time scales may be forced by orographic or other landscape forcing rather than forced by the thermal circulations.

A more quantitative comparison of the observed and simulated spectral distribution is provided in Figures 10 and 11. The spectral power in each band is normalized by the total power for each site. At 10 m AGL, it can be noted that the sites are grouped into a group of three (JCF, DDB and XCH), and one isolated site (CSC). Sites of JCF, DDB and XCH contain about 66% of their power in the LTD band and about 25% in the subdiurnal periods, whereas CSC contains 81.6% of its power in the LTD band and 16.2% in the subdiurnal period. Only 3% of the spectral power is attributed to the diurnal band. The results from W3km classify the sites of JCF, CSC and XCH in complex terrain as a category, leaving the DDB site at flat terrain as the isolated one. The W3km spectra have more power in the LTD band and less power in the subdiurnal bands. W1km reduces the power in the LTD band by 1–3%. The power in the diurnal and subdiurnal bands is increased by 1–5% and 1%, respectively. Finally, results from W3km/C100m and W1km/C100m are similar and present the largest power in the LTD band and the smallest power in the subdiurnal band at the site of CSC. This feature is consistent with the observed. Similar results are shown in Figure 11 for wind speed at 60 m AGL.

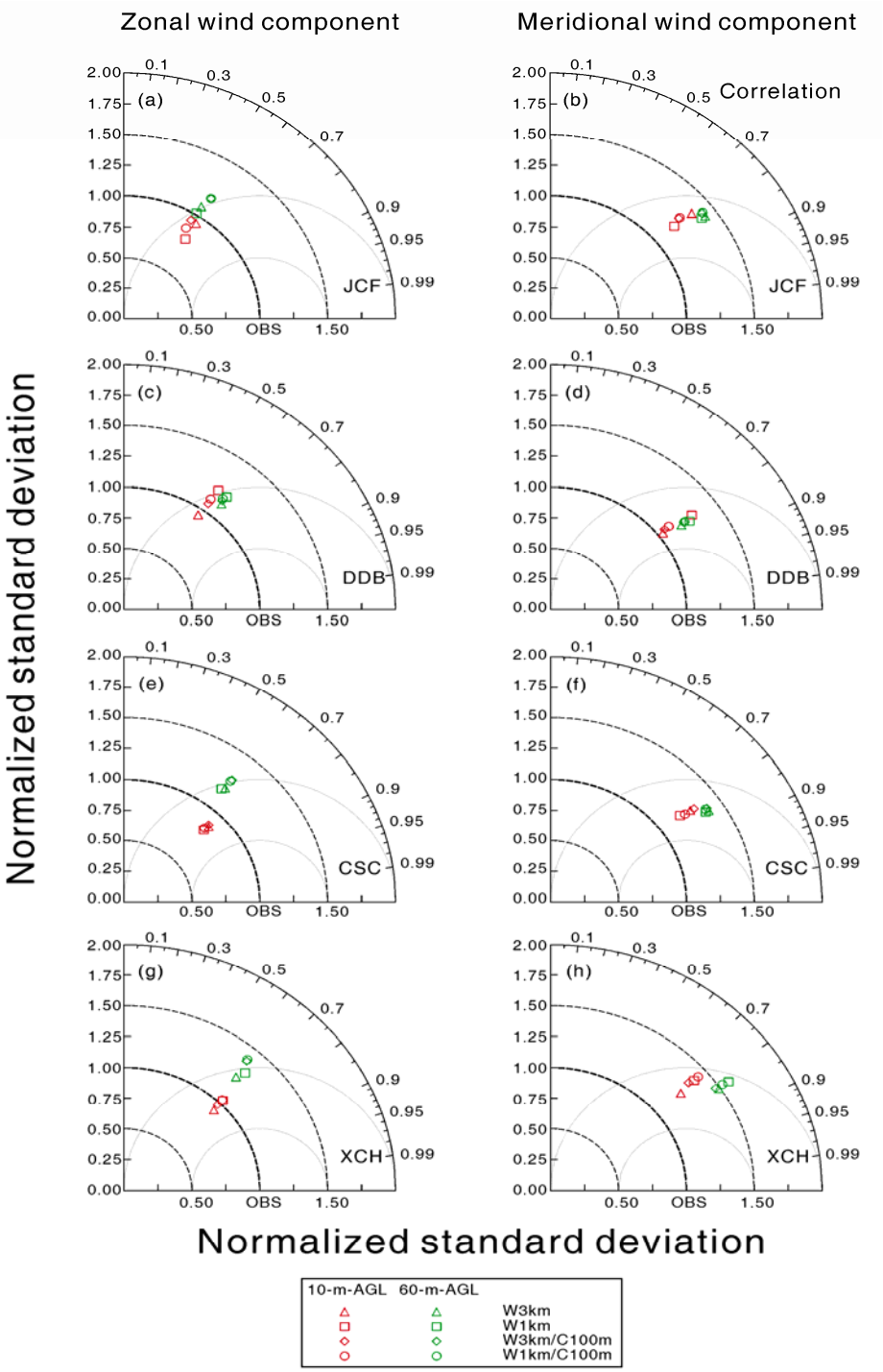

Figure 6. Normalized Taylor diagrams comparing the (left) zonal and (right) meridional wind components at each site.

3.3 *Spatial variability*

Investigating the spatial variability of the simulated wind field is important because one of the major potential benefits of the WRF/CALMET modeling system is for capturing the effects of finer scale terrain on the wind field. Figure 12 illustrates the 30-m-AGL wind field obtained by W1km and W1km/C100m, respectively. Although the 1-km WRF can develop the regional wind regime, it could not resolve the detailed terrain structure and flow variation as shown in Figure 12a. Wind speed and direction are almost uniform on the 1-km grid. On the other hand, the 100-m CALMET provides more detailed terrain and wind field structures within the local region as shown in Figure 12b. The prevalent wind pattern is defined by both the northeast wind and the speed-up and sheltering by hills. For example, the blocking effects of hill C, and flows around hill C were clearly reproduced by CALMET. The corresponding channel effects between hills B and C, as well as between hills D and C are also captured. The wind speed exhibits significant spatial variation

on the 100-m grid, characterized by wind speed maxima around hilltops associated with slope flows. In addition, two primary wind speed minima are located between hills A and C, associated with the convergence of flows on the downwind side of hill C and the blocking effects on the upwind side of hill A. These results indicate that the combined WRF/CALMET system shows great skill at deriving local structure of wind field in a complex terrain.

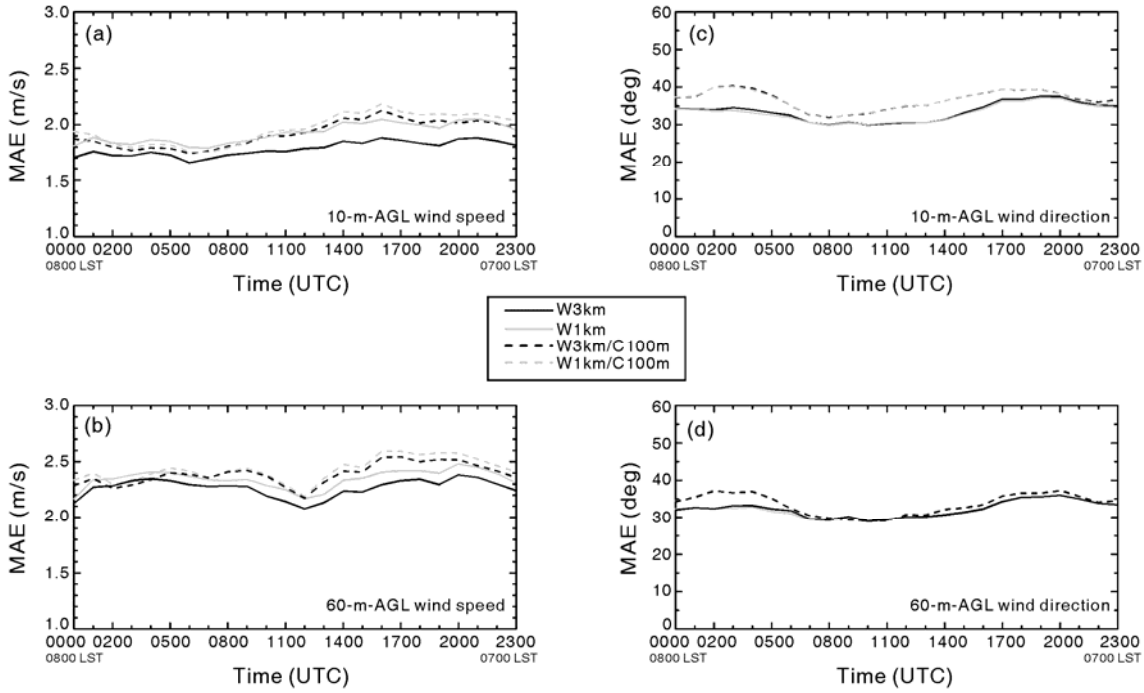

Figure 7. Diurnal characteristics of the average MAE for wind speed (left panels) and wind direction (right panels) in the 1-year period.

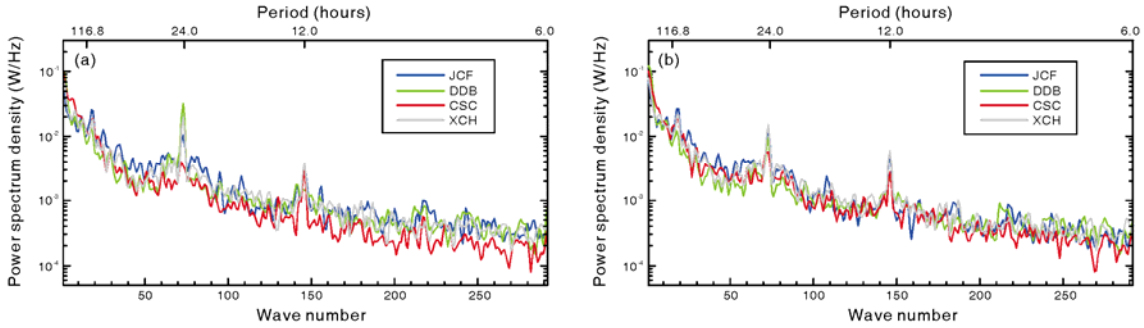

Figure 8. Spectral power distribution as a function of period for the observed wind speed at the four sites at (a) 10 m AGL and (b) 60 m AGL.

4 CONCLUSIONS AND DISCUSSION

In this study, a combined WRF/CALMET modeling system was developed to generate wind estimates on the hilly Hailing Island. WRF was run in a one-way nested mode with grid spacing of 27, 9, 3 and 1 km. CALMET was run with grid spacing of 100 m, coupled offline to the WRF model. Simulated winds were first compared with the time series of observations at 4 sites by traditional verification scores. Decreasing grid spacing from 3 km to 100 m provides more detailed topographic features, but there is no corresponding improvement indicated by the correlation coefficient. The MAEs actually increase somewhat as the grid spacing decreases. The traditional statistical scores are incapable of showing a positive impact of increasing horizontal resolution.

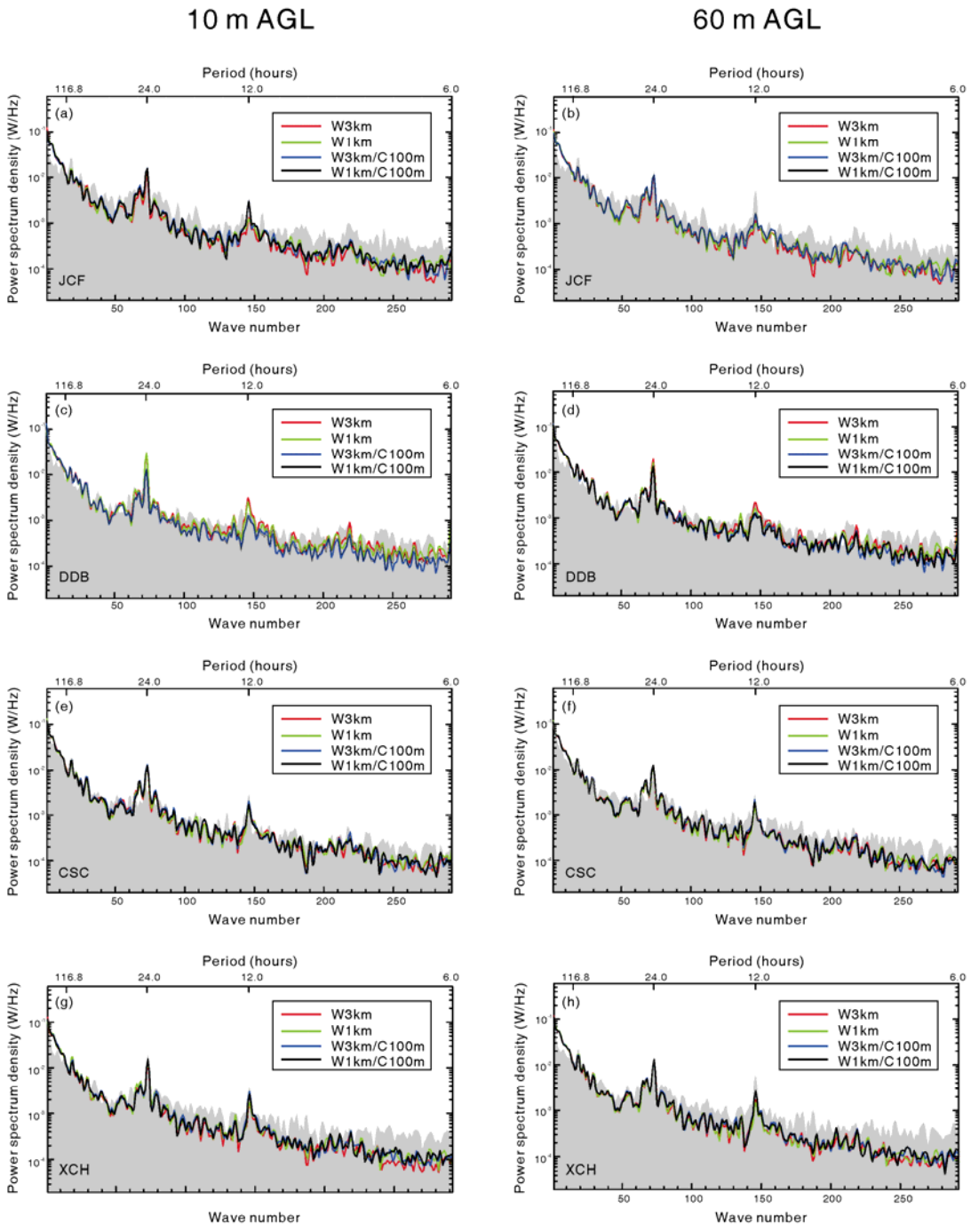

Figure 9. Observed versus simulated power spectra for the wind speed at the four sites. The shaded areas represent the observed spectra.

Similar results have been found in the study of Ludwig et al.[8], in which the diagnostic wind model (Winds on Critical Streamline Surfaces, WOCSS) was driven with forecasts from the Coupled Ocean-Atmosphere Mesoscale Prediction System (COAMPS) to obtain detailed near-surface wind forecasts with 3-km horizontal spacing. It was pointed out that the diagnostic model was developed to treat terrain effects on atmospheric flows during stable conditions. The unstable conditions were not what the model was designed to address. The relatively long analytical periods might span both types of conditions and blur the results. The performance of CALMET under very specific weather situations can be investigated for future study. Such investigations would likely give clues to improve the physics in CALMET to address some constraints imposed on the flow by the terrain under different weather situations.

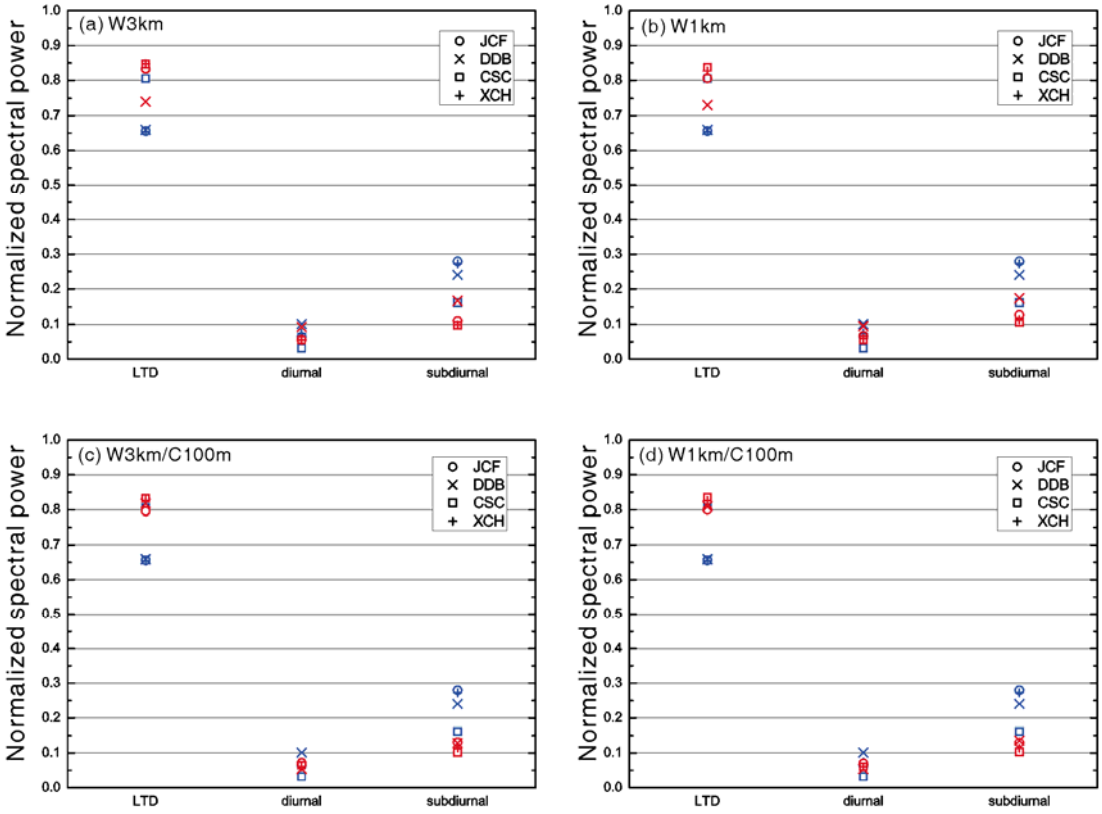

Figure 10. Observed (blue) versus simulated (red) spectral power at 10 m AGL in each band normalized by the total power.

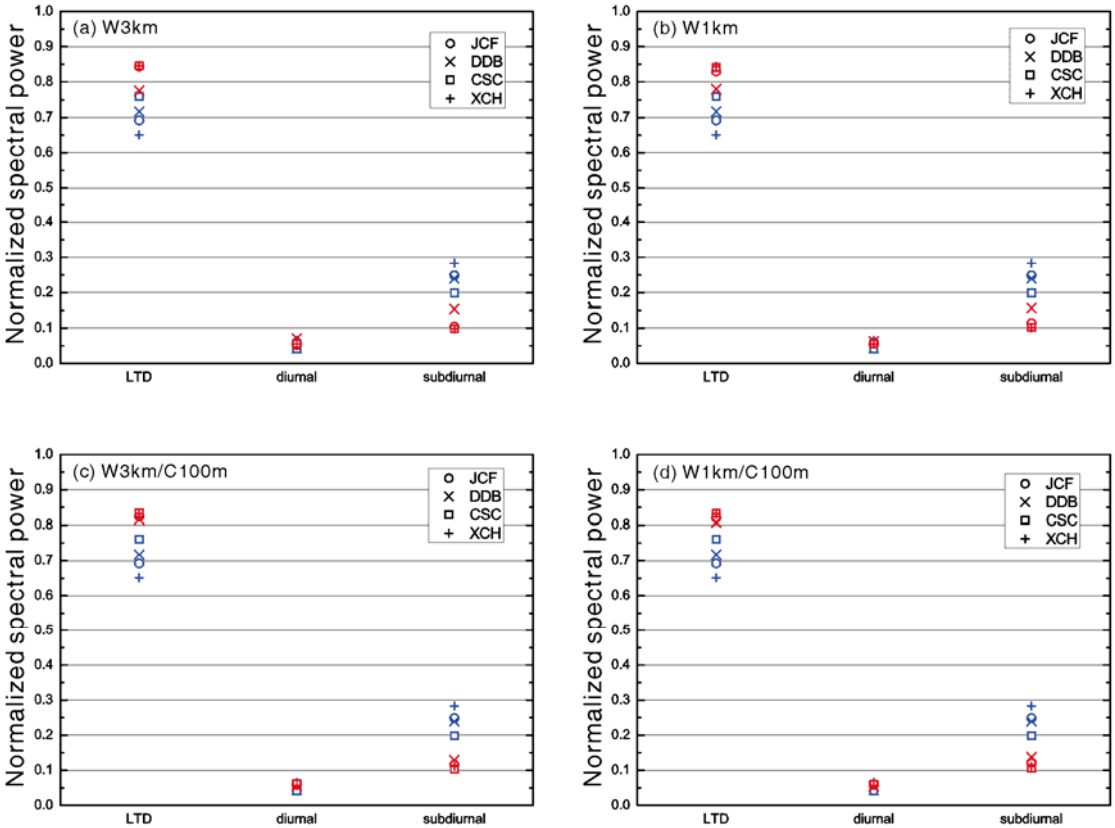

Figure 11. Same as Figure 10 but at 60 m AGL.

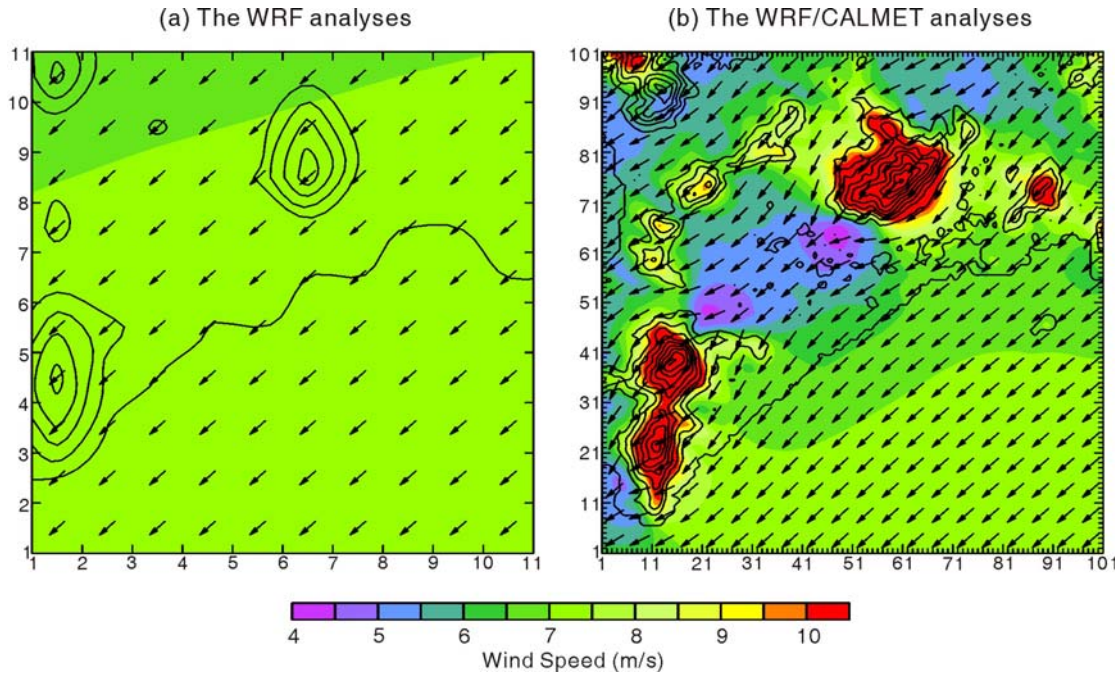

Figure 12. Comparison of wind fields between (a) the W1km analyses and (b) the W1km/C100m analyses (see Figure 2 for locations). The average wind fields are calculated at 30 m AGL from September 12 to November 17, 2003. The shades of color represent the mean wind speed, and the vectors represent the prevailing wind direction. The isopleths represent the terrain height with intervals of 40 m.

A more physical insight is attempted through a comparison of the observed and simulated wind time-series in the spectral domain. The WRF model with 3-km grid spacing tends to group sites in complex terrain (JCF, CSC and XCH) into a category, and isolate the site (DDB) at flat terrain. Results from the 1-km WRF were similar to that from the 3-km WRF. More realistic spectral distributions are presented by the 100-m CALMET results. It is encouraging of the WRF/CALMET modeling system to show positive impact in simulating highly variable wind field in complex terrain. The CALMET model could add value to the simulations for the near-surface wind field, suggesting that the subdiurnal scale flows relating to the local topography could be generated to some extent.

An intercomparison indicates that the potential benefit of the high-resolution WRF/CALMET system is great. Increasing horizontal resolution does provide more realistic simulated wind fields. Wind flows around hills, slope flows and blocking effects of hills are clearly presented in the CALMET analyses. Wind speed maxima are generally associated with hilltops, and the minima are found on the upwind side of hills due to the blocking effects and on the downwind side of hills as the convergence of flows.

The overall performance of the WRF/CALMET system is good in deriving high-resolution wind field in complex terrain. Developing alternative evaluation methodology would be an important extension to the current work. It is expected that more physical clues can be uncovered in the process of developing the WRF/CALMET system.

Acknowledgement: We thank Prof. ZHAO Ming and Prof. YUAN Hui-ling for their helpful discussions.

REFERENCES:

[1] KLINK K. Trends and interannual variability of wind speed distributions in Minnesota [J]. J. Climate, 2002, 15: 3311-3317.
[2] JIMÉNEZ P A, GONZÁLEZ-ROUCO J F, MONTÁVEZ J P, et al. Surface wind regionalization in complex terrain [J]. J. Appl. Meteor. Climatol., 2008, 47: 308-325.
[3] JIMÉNEZ P A, GONZÁLEZ-ROUCO J F, MONTÁVEZ J P, et al. Climatology of wind patterns in the northeast of the Iberian Peninsula [J]. Int. J. Climatol., 2009, 29: 501-525.
[4] WAN H, WANG X L, SWAIL V R. Homogenization and trend analysis of Canadian near-surface wind speeds [J]. J. Climate, 2010, 23: 1209-1225.
[5] RIFE D L, DAVIS C A, LIU Y B, et al. Predictability of low-level winds by mesoscale meteorological models [J]. Mon. Wea. Rev., 2004, 132: 2533-2569.
[6] ŽAGAR N, ŽAGAR M, CEDILNIK J, et al. Validation of mesoscale low-level winds obtained by dynamical downscaling of ERA40 over complex terrain [J]. Tellus, 2006, 58A: 445-455.
[7] JIMÉNEZ P A, GONZÁLEZ-ROUCO J F, GARCÍA-BUSTAMANTE E, et al. Surface wind regionalization over complex terrain: Evaluation and analysis of a high-resolution WRF simulation [J]. J. Appl. Meteor. Climatol., 2010, 49: 268-287.
[8] LUDWIG F L, MILLER D K, GALLAHER S G. Evaluating a hybrid prognostic-diagnostic model that improves wind forecast resolution in complex coastal topography [J]. J. Appl. Meteor. Climatol., 2006, 45: 155-177.
[9] CHANDRASEKAR A, PHILBRICK C R, CLARK R, et al. Evaluating the performance of a computationally efficient MM5/CALMET system for developing wind field inputs to air quality models [J]. Atmos. Environ., 2003, 37: 3267-3276.

[10] JACKSON B, CHAU D, GURER K, et al. Comparison of ozone simulations using MM5 and CALMET/MM5 hybrid meteorological fields for the July/August 2000 CCOS episode [J]. Atmos. Environ., 2006, 40: 2812-2822.
[11] YIM S H L, FUNG J C H, LAU A K H, et al. Developing a high-resolution wind map for a complex terrain with a coupled MM5/CALMET system [J]. J. Geophys, Res., 2007, 112:D05106. doi:10.1029/2006JD007752.
[12] SKAMAROCK W C, KLEMP J B, DUDHIA J, et al. A description of the advanced research WRF version 3 [R]. 2008, NCAR Tech. Note TN-475 +STR, 125pp.
[13] POWERS J G. Numerical prediction of an Antarctic severe wind event with the Weather Research and Forecasting (WRF) model [J]. Mon. Wea. Rev., 2007, 135: 3134-3157.
[14] DAVIS C, WANG W, CHEN S S, et al. Prediction of landfalling hurricanes with the advanced hurricane WRF model [J]. Mon. Wea. Rev., 2008, 136: 1990-2005.
[15] BAO J W, MICHELSON S A, PERSSON P O G, et al. Observed and WRF-simulated low-level winds in a high-ozone episode during the Central California Ozone Study [J]. J. Appl. Meteor. Climatol., 2008, 47: 2372-2394.
[16] BUKOVSKY M S, KAROLY D J. Precipitation simulations using WRF as a nested regional climate model [J]. J. Appl. Meteor. Climatol., 2009, 48: 2152-2159.
[17] RUIZ J J, SAULO C, NOGUÉS-PAEGLE J. WRF model sensitivity to choice of parameterization over South America: Validation against surface variables [J]. Mon. Wea. Rev., 2010, 138: 3342-3355.
[18] HONG S Y, DUDHIA J, CHEN S H. A revised approach to ice microphysical processes for the bulk parameterization of clouds and precipitation [J]. Mon. Wea. Rev., 2004, 132: 103-120.
[19] KAIN J S. The Kain-Fritsch convective parameterization: An update [J]. J. Appl. Meteor., 2004, 43, 170-181.
[20] DUDHIA J. Numerical study of convection observed during the Winter Monsoon Experiment using a mesoscale two-dimensional model [J]. J. Atmos. Sci., 1989, 46: 3077-3107.
[21] MLAWER E J, TAUBMAN S J, BROWN P D, et al. Radiative transfer for inhomogeneous atmospheres: RRTM, a validated correlated-k model for the longwave [J]. J. Geophys. Res., 1997, 102, 16663-16682.
[22] HONG S Y, NOH Y, DUDHIA J. A new vertical diffusion package with an explicit treatment of entrainment processes [J]. Mon. Wea. Rev., 2006, 134: 2318-2341.
[23] PAN Z, TAKLE E, GUTOWSKI W, et al. Long simulation of regional climate as a sequence of short segments [J]. Mon. Wea. Rev., 1999, 127: 308-321.
[24] QIAN J H, SETH A, ZEBIAK S. Reinitialized versus continuous simulations for regional climate downscaling [J]. Mon. Wea. Rev., 2003, 131: 2857-2874.
[25] LO J C F, YANG Z L, PIELKE R A. Assessment of three dynamical climate downscaling methods using the Weather Research and Forecasting (WRF) model [J]. J. Geophys. Res., 2008, 113:D09112. doi:10.1029/2007JD009216.
[26] SCIRE J S, ROBE F R, FERNAU M E, et al. A user's guide for the CALMET meteorological model (version 5) [R]. 2000, Earth Tech, Inc., 332 pp.
[27] TAYLOR K E. Summarizing multiple aspects of model performance in a single diagram [J]. J. Geophys. Res., 2001, 106: 7183-7192.
[28] MASS C F, OVENS D, WESTRICK K, et al. Does increasing horizontal resolution produce more skillful forecasts? [J]. Bull. Amer. Meteor. Soc., 2002, 83: 407-430.
[29] GHIL M, ALLEN M R, DETTINGER M D, et al. Advanced spectral methods for climatic time series [J]. Rev. Geophys., 2002, 40:1003. doi:10.1029/2000RG000092.

Citation: LU Yi-xiong, TANG Jian-ping, WANG Yuan et al. Validation of near-surface winds obtained by a hybrid WRF/CALMET modeling system over a coastal island with complex terrain. *J. Trop. Meteor.*, 2012, 18(3): 284-296.